*Original Research*

# Estimation of Driver Drowsiness Using Blood Perfusion Analysis of Facial Thermal Images in a Driving Simulator

Masoumeh Tashakori*, Ali Nahvi, Azadeh Shahidian,
Serajeddin Ebrahimian-Hadi kiashari, Hamidreza Bakhoda

*Department of Mechanical Engineering, School of Mechanical Engineering, Khajeh Nasir Toosi University of Technology, Tehran, Iran*

Received: 01 Jun. 2018 Accepted: 05 Jul. 2018

## Abstract

**Background and Objective:** Driver drowsiness is a major cause of fatal driving accidents worldwide, which can be prevented by an early detection. Driver drowsiness results in reduction of blood flow and change in facial thermal patterns. In this paper, a drowsiness detection system was designed to estimate the level of drowsiness by analyzing facial skin temperature patterns.

**Materials and Methods:** 12 subjects drove on a highway in a driving simulator, while their facial temperature image was captured by a thermal camera. The subjects' drowsiness levels were independently estimated by the observer rating of drowsiness (ORD) method. Facial blood vessels were located by a four-step algorithm and tracked in each frame. The mean value of the pixel intensities of the facial blood regions formed a sequence of data. Variations of facial skin temperature signals were investigated for three main blood vessels.

**Results:** Facial skin temperature decreased at three levels of sleepiness from wakefulness to extreme drowsiness. Temperature near the supratrochlear, angular, and facial arteries decreased by 0.54 ºC, 0.33 ºC, and 0.32 ºC from wakefulness to extreme drowsiness, respectively. All subjects except one experienced skin temperature decrease from wakefulness to extreme drowsiness.

**Conclusion:** It was shown that the drivers' facial blood vessels temperature decreased as the level of drowsiness increased. Driver drowsiness can be detected by monitoring the change in the facial skin temperature signal during driving. Facial thermal imaging is a promising non-intrusive method to detect driver drowsiness.



**Keywords:** Sleep; Skin temperature; Thermography; Driving simulator

**Citation:** Tashakori M, Nahvi A, Shahidian A, Ebrahimian-Hadikiashari S, Bakhoda H. **Estimation of Driver Drowsiness Using Blood Perfusion Analysis of Facial Thermal Images in a Driving Simulator.** J Sleep Sci 2018; 3(3-4): 45-52.

## Introduction

Driver drowsiness is a major cause of driving accidents worldwide. Drowsiness decreases awareness and reaction time, impairs judgment, and increases the risk of human errors leading to fatalities and injuries (1). Factors such as sleep deprivation, work schedules, sleep disorders, time of day, circadian rhythm, and long hours behind the wheel in monotonous driving environments affect driver drowsiness (2). Drowsiness detection systems are one of the promising methods to decrease driving accidents.

Drowsiness detection systems are either non-invasive or invasive. Non-invasive systems monitor driver's facial features and vehicle dynamics variables. Invasive systems monitor driver's physiological signals (3).

Facial features are often extracted by image processing to estimate the level of drowsiness. During drowsiness, facial appearance changes, particularly eyes, head, and mouth. Facial features detection systems are often sensitive to the ambient light. Vehicle dynamics systems suffer from low processing speed and are dependent on vehicle characteristics. Physiological signals are accu-

**** Corresponding author**: M. Tashakori, School of Mechanical Engineering, Khajeh Nasir Toosi University of Technology, Tehran, Iran*
*Tel: +98 918 901 6020, Fax: +98 21 88674748*
*Email: tashakori_1992@email.kntu.ac.ir*

rate in determining the driver's status, and are usually used to validate other systems or used in clinical studies. Because of the invasive nature of most physiological systems, they are not suitable for in-vehicle monitoring (4).

In recent decades, infrared thermal imaging has been introduced as an ideal technology for monitoring physiological conditions. This method is not affected by the ambient light and the headlights of the approaching vehicles (5). Thermal imaging is a non-invasive monitoring method and has attracted many researchers to use it in medicine, biometrics, and machine vision. Wu et al. extracted the thermal pattern of face using thermal imaging under alcohol consumption (6).

The results indicated increased temperature of the face. In another study, Gault et al. extracted human facial vasculature from thermal imaging and estimated human's heart rate based on a small number of thermal video frames (7). In another study conducted by Buddharaju et al., blood vessels of face were extracted by image processing techniques using thermal imaging (8).

A few studies have been conducted on the relationship between sleepiness and body temperature. Bando et al. studied changes in the forehead skin temperature at both right and left sides as the level of drowsiness increased (9). The results showed that the forehead temperature at both sides decreased from wakefulness to extreme drowsiness by 0.1 ºC, on average. However, they did not report the difference between skin areas near or far away from the supratrochlear arteries. A few studies have investigated the relationship between sleepiness and the core body temperature. Krauchi et al. obtained a relationship between the heat loss and sleepiness (10). They showed that the core body temperature decreased as sleepiness increased, but the skin temperature at the foot and the stomach areas increased as the sleepiness increased. Gradisar and Lack measured the circadian rhythm relationship between the distal skin and the core body temperatures and sleepiness (11). They found an inverse relationship between core body temperature and sleepiness, but the finger temperature rose as sleepiness increased. Moradi et al. studied sleepiness and changes in vital signs among the clinical shift workers (12). The results showed that sleepiness had an inverse correlation with the core body temperature and the blood pressure.

In this paper, variations of drivers' facial temperature were investigated through thermal imaging. The blood vessels are one of the facial regions in thermal videos that show the physiological state of the subjects (8).

This paper helps researchers to indirectly monitor drivers' blood perfusion and estimate the level of drowsiness. Facial skin temperature is closely related to the underlying blood vessels; thus, by obtaining a thermal map of the human face, we can extract the distribution of the blood vessels beneath the skin. The mean facial temperatures of skin above three main blood vessels are derived in 2-minute intervals. Three levels of drowsiness are estimated by the observer rating of drowsiness (ORD) method (13). The aim of this study was to estimate the level of driver's drowsiness by analyzing facial skin temperature as a non-invasive monitoring method. This monitoring method has a potential to warn driver's sleepiness at the moderate level of drowsiness long before the last stage of drowsiness.

## Materials and Methods

Driving tests were performed in a driving simulator to study the temperature variations of facial blood vessels at three levels of wakefulness. An experimental protocol and a driving scenario were designed to provide all stages of drowsiness for the subjects. Data acquisition tools included a thermal camera to measure facial temperature and a night vision camera to monitor the driver. Drowsiness levels were estimated by the ORD method (13).

***Signal extraction:*** To extract the facial skin temperature signal, a thermal camera was used to capture facial thermal image. Variations of temperature were monitored in three skin regions covering three facial blood vessels, i.e., facial artery, angular artery, and supratrochlear artery. A robust algorithm was used to identify and track the regions continuously. These regions were identified and located automatically in the initial frames of the video and then tracked in the subsequent frames to record temperature variations during driving.

***Extraction of blood vessels' region:*** Facial skin temperature is related to the underlying blood vessels. The pattern of the blood vessels below the skin could be extracted by thermal camera. There is a thermal equilibrium between the face and the environment. The core body temperature was

controlled through several processes, including sweat production and the rate of blood flowing through the skin.

Studies provided an algorithm for extracting facial thermal signature network from the thermal image (7). The thermal signature extraction process consists of four main steps: face segmentation, noise removal, image morphology, and post-processing.

The segmentation process was achieved by implementing the Bayesian segmentation scheme on the subject's facial image. The human face's tissue consists of two parts. One part was tissue areas with rich vasculature and another part with sparse vasculature. Therefore, the thermal image could be described by a bimodal temperature distribution with the background being the "cold" sparse vasculature and the foreground being the "hot" rich vasculature. Figure 1(a) shows the segmentation process.

The unwanted noise was removed to enhance the image for further processing. An anisotropic diffusion filter (14) was applied to the thermal image to reduce the image noise without removing significant parts of the image content. The anisotropic diffusion filtering was an iterative process which continued until a sufficient degree of smoothing was obtained.

Morphological operators were applied to the diffused image. The blood vessels were assumed as tubule-like structures running along the length of the face. For this purpose, opening and top-hat segmentation were used. The top-hat segmentation was defined as the difference between the input image and its opening. Figure 1(b) indicates morphological operators.

The final step for extracting the thermal signature was post-processing. Post-processing was a process for reducing foreground regions in an image to a skeletal remnant by throwing away most of the original foreground pixels. Figure 1(c) illustrates post-processing and pattern of the extracted blood vessels. Then, the three blood vessels at the right side of the face, i.e., supratrochlear, angular, and facial arteries, were localized by the algorithm. These target regions were located in the forehead alongside the nose and the chin, as shown in figure 1(d).

***Tracking regions of interest:*** Facial skin temperature in the target regions were tracked. Many studies have been conducted to track the target regions in non-thermal visible images (15). Some of these tracking methods could also be applied for thermal images.

The spatio-temporal context learning (STCL) method was used in this study. This method is based on modeling the statistical correlation of low-level features of an image such as color intensity. The tracking region was localized by extracting spatio-temporal relationship between the target and the surrounding regions based on the Bayesian structure. In this method, tracking target regions was performed using a confidence map (16).

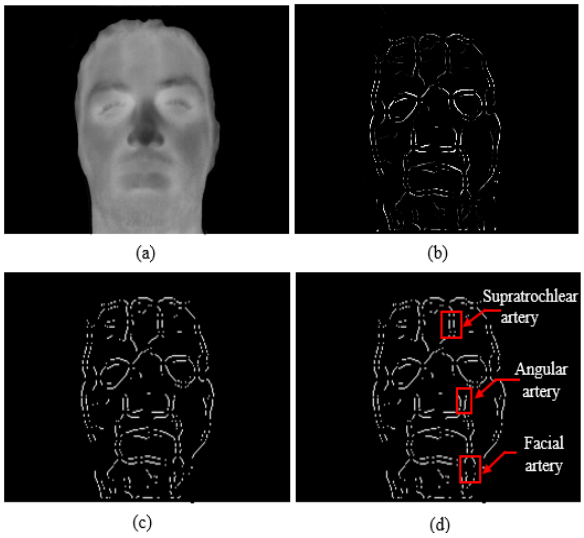


**Figure 1.** Face segmentation (a), image morphology (b), post-processing (c), target regions (d)

After localizing target regions in frame #1, target regions in the subsequent frames were tracked. In each frame, the mean pixel intensities of the target regions were taken as signal values. This algorithm was applied for all three regions of the three main blood vessels. Figure 2(a) illustrates performance of the tracker in the target region of the right supratrochlear artery when the driver is wakeful. In figures 2(b) and 2(c), the tracking algorithm tracks this target region despite head tilting. Figures 2(d), 2(e), and 2(f) show that the tracking algorithm follows the region of the right angular artery despite thermal fluctuating disturbance due to respiration. In figures 2(g), 2(h), and 2(i), the tracking algorithm tracks the right facial artery region despite combined head tilting and nodding.

Raw signals needed to be cleaned by removing high-frequency noise. A fourth-order Butterworth low-pass filter was applied to the signal with a cutoff frequency of 0.005 Hz. The high-frequency noise was due to the head movement or the air thermal fluctuations.

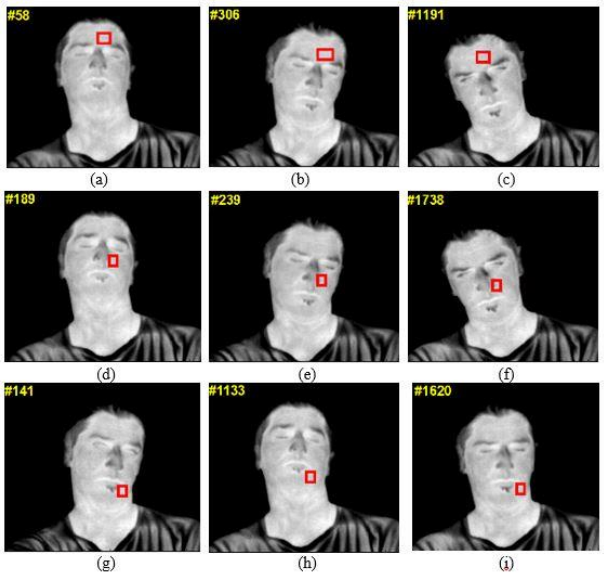


**Figure 2.** The tracking algorithm tracks the right supratrochlear artery despite head tilting (a), (b), and (c); the tracker in the right angular artery is robust against thermal fluctuating disturbances due to respiration (d), (e), and (f); and the tracker follows the right facial artery despite combined head tilting and nodding (g), (h), and (i)

***Driving simulator:*** Experiments were conducted in a driving simulator. The driving simulator was built at the Virtual Reality Laboratory of Khajeh Nasir Toosi University of Technology, Tehran, Iran, with the one-quarter body of a real sedan as shown in figure 3.

A 700-W AC servo motor exerted the road lateral force on the steering wheel. The pedals were equipped with potentiometers to measure driver inputs. The simulated vehicle had 14 degrees of freedom (DF) and the sampling rate was about 30 Hz.

**Figure 3.** Nasir driving simulator

***Driver monitoring tools:*** A thermal camera and a night vision camera were used to record thermal and near infrared images of the driver's face. The thermal camera dimension was 195 × 105 × 121 mm. The thermal image had a spatial resolution of 640 × 480 and a thermal resolution of 30 m-Kelvin. The drivers' drowsiness level was estimated from the video of the night vision camera. Also, five sensors were used to record temperature and humidity of the environment with the sampling rate of 0.2 Hz. Figure 4 illustrates location of the two cameras.

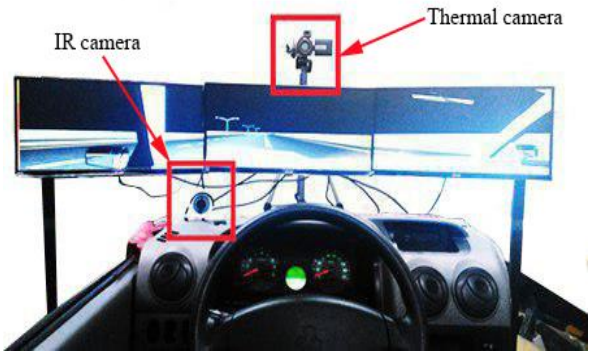


**Figure 4.** Placement of thermal and infrared cameras (17)

***Test participants:*** The participants were 12 male subjects. They aged between 23 and 29 years with the mean body mass index (BMI) of 25.6 kg/m$^2$. The subjects were volunteers and signed consent forms to do the experiments. The participants did not have any history of medical problems including cardiovascular diseases (CVDs). All subjects had driver's license and driving experience of at least 3 years. The tests were held during the night between 10 pm and 6 am at a dark room. Figure 5 shows the facial thermal images of the participants.

**Figure 5.** Thermal images of the subjects

Before the start of the test, the drivers got familiar with the driving simulator by having a 15-minute drill session. All of the 12 subjects were asked to avoid sleeping and eating stimulants on the day before the test night and reduce their sleeping time down to 4 hours in each 24 hours during the last three days leading to the test night. The experimental protocol was approved by the *Khajeh Nasir Toosi* University of Technology in accordance with the Declaration of Helsinki.

***Driving scenario:*** The road was a quasi-circular loop with the mean radius of 10 km as shown in figure 6(a). The three-lane highway had a shoulder on the right and a guardrail on the left as shown in figure 6(b). There were no obstacles or vehicles along the way to prevent driver distraction. The surrounding areas of the road were monotonous and boring to increase drowsiness.

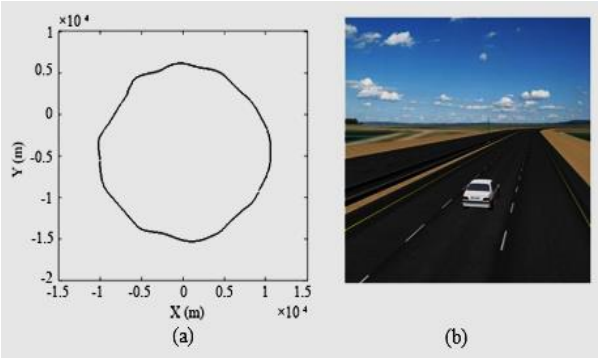


**Figure 6.** The quasi-circular map of the three-lane highway (a), the graphical view of the road (b)

The drivers were required to drive with the speed of 80 km/h. The vehicle departed off the lane when the driver became drowsy. Therefore, the drivers were asked to drive on the middle lane to have enough time before they reach the shoulder or hit the guardrail. The test ended when the car departed off the road. Each test continued for at most 2 hours.

***Validation:*** The drivers' drowsiness level was validated by the ORD method (13). Three researchers monitored drivers' face and behavior by inspecting the video recorded from a night vision camera. A number from 1 to 5 was used to score wakefulness to extreme drowsiness based on changes in certain facial and behavioral features.

## Results

Signals of drivers' skin temperature in the three target regions were extracted. The demographic characteristics of the subjects and the environment data are shown in table 1. Figure 7 shows temperature in the three target regions in wakeful, moderately drowsy, and extremely drowsy states for one of the twelve subjects during a two-minute interval. As shown, temperature signal at all the three regions related to the three main blood vessels dropped from wakefulness to extreme drowsiness.

The temperature of three target regions was analyzed at three stages of drowsiness after applying a low-pass filter for all 12 subjects. Three levels of drowsiness were considered in 2-minute intervals including wakeful (ORD = 1), moderately drowsy (ORD = 3), and extremely drowsy (ORD = 5). Due to metabolic and physiological differences among the subjects, the amount of decrease in the temperature of the target regions varied.

**Table 1.** Demographic characteristics of the subjects and the environment data

| Subject number | Age (year) | Height (m) | Weight (kg) | BMI (kg/m$^2$) | Room humidity (%) (SD) | Room temperature (ºC) (SD) |
|---|---|---|---|---|---|---|
| 1 | 25 | 1.79 | 80 | 24.96 | 46.15 (0.34) | 23.78 (0.17) |
| 2 | 23 | 1.83 | 88 | 26.27 | 44.67 (0.25) | 24.29 (0.32) |
| 3 | 24 | 1.81 | 75 | 22.89 | 45.36 (0.06) | 24.30 (0.40) |
| 4 | 25 | 1.86 | 80 | 23.12 | 47.35 (0.12) | 24.37 (0.08) |
| 5 | 25 | 1.75 | 75 | 24.48 | 41.82 (0.12) | 23.51 (0.16) |
| 6 | 25 | 1.73 | 83 | 27.73 | 43.25 (0.09) | 23.68 (0.03) |
| 7 | 26 | 1.71 | 85 | 29.06 | 44.12 (0.23) | 22.86 (0.11) |
| 8 | 22 | 1.70 | 68 | 23.52 | 46.62 (0.11) | 23.12 (0.30) |
| 9 | 28 | 1.88 | 80 | 22.63 | 43.61 (0.09) | 22.70 (0.33) |
| 10 | 25 | 1.82 | 90 | 27.17 | 45.74 (0.20) | 22.80 (0.30) |
| 11 | 27 | 1.72 | 80 | 27.04 | 43.15 (0.13) | 22.08 (0.08) |
| 12 | 25 | 1.89 | 100 | 27.99 | 44.95 (0.25) | 23.28 (0.12) |
| Mean | 25 | 1.79 | 82 | 25.57 | 44.73 (0.16) | 23.40 (0.17) |

SD: Standard deviation; BMI: Body mass index

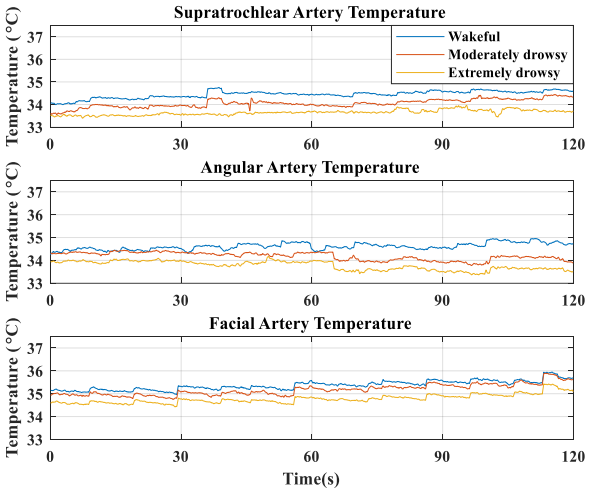


**Figure 7.** Temperature at three target regions for one driver in a 2-minute interval for wakeful, moderately drowsy, and extremely drowsy states

All subjects except subject #6 showed skin temperature decrease from wakefulness to extreme drowsiness. Figure 8 illustrates facial skin temperature in the three target regions of blood vessels at three levels of drowsiness for each subject.

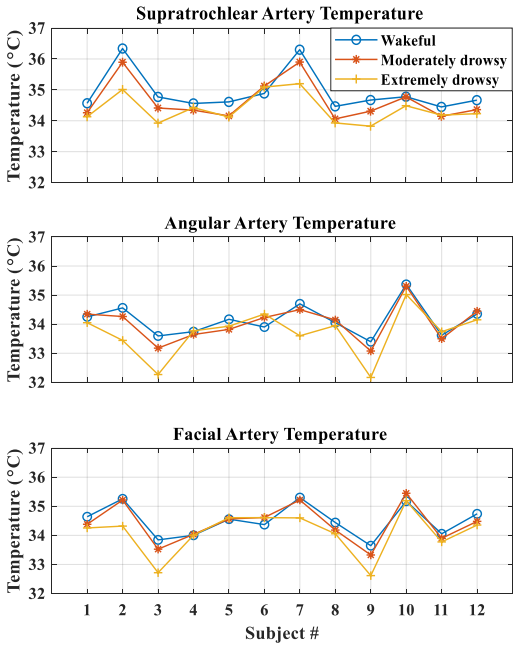


**Figure 8.** Integrated temperature signals of all 12 subjects in a box plot at the three regions for three levels of drowsiness

As shown in figure 9, the mean temperature of the three main blood vessels decreased at three levels of sleepiness from wakefulness to extreme drowsiness. At the moderate level of drowsiness, the median of the target region of the supratrochlear artery temperature decreased by 0.31 ºC and decreased further by 0.23 ºC at extreme drowsiness. Also, the median of the target region of the angular artery temperature had a tiny decrease of 0.05 ºC at moderate drowsiness, but it had a more noticeable drop of 0.28 ºC from moderate to extreme drowsiness. The median of the target region of the facial artery temperature decreased by 0.20 ºC at the moderate drowsiness and by 0.12 ºC at the extreme drowsiness.

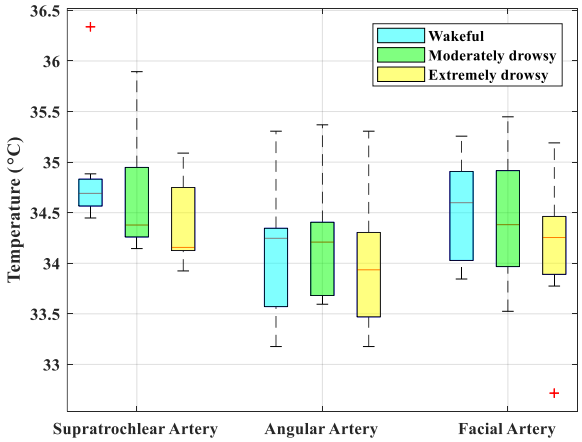


**Figure 9.** Box plot of the mean temperature of supratrochlear artery, angular artery, and facial artery regions in 2-minute intervals during wakefulness, moderate drowsiness, and extreme drowsiness

## Discussion

In this study, a thermal camera was used to extract drivers' facial skin temperature during drowsiness. Facial thermal signature pattern was extracted from the thermal image. The target regions were identified and tracked in each frame and the mean temperature of the target regions was considered as the temperature signal. The facial skin temperature signal was derived in two-minute intervals.

The facial skin temperatures of 12 drivers were extracted in three levels of drowsiness. The drowsiness levels of drivers were determined using the ORD method. The results showed that the facial skin temperature of the subjects decreased from wakefulness to moderate and extreme drowsiness in skin areas covering the main arteries. From wakefulness to extreme drowsiness, the mean temperature difference was 0.54 ºC, 0.33 ºC, and 0.32 ºC for supratrochlear, angular, and facial arteries. According to the results, drowsy drivers can be detected by monitoring the change of facial

skin temperature signal during driving at these areas, especially the skin area covering the supratrochlear artery.

Several studies have been conducted on the relationship between sleepiness and the core body temperature. However, there is still no study on the relationship between the skin temperature covering the main blood vessels and sleepiness. Variations of forehead temperature due to drowsiness had been studied by Bando et al. (9). They measured facial temperature of seven subjects at the two sides of the forehead by thermography. The results indicated that the forehead temperature decreased by an average of 0.1 ºC at the both sides of the face as the level of drowsiness increased. But, they did not consider the main blood vessels regions. A major difference from this previous work is that the present paper extracted skin temperatures in the regions covering the main blood vessels of the forehead. We showed a significant temperature decline of 0.54 ºC from wakefulness to extreme drowsiness. The present work also presented the results for two other regions of the face just above the facial and angular arteries.

Future researches can be conducted for detection of drowsiness at other facial areas and also for patients with sleep disorders. Change of skin temperature during drowsiness at areas away from the main arteries can enrich drowsiness detection. Study of facial skin temperature change during drowsiness for patients with narcolepsy and apnea may result in significant findings. Also, facial skin temperature can be analyzed to detect CVDs. CVDs affect facial vessel temperature patterns and may be used as a diagnostic tool (18).

Differences in individuals and the ambient temperature may deviate the results from a uniform pattern. Metabolism and physiology of the subjects may result in variations in the pattern of temperature decrease during drowsiness. For example, subject #6 showed skin temperature increase from wakefulness to extreme drowsiness unlike other 11 subjects. In real driving, the ambient temperature varies over time.

The experiments conducted in this study were held in a controlled and steady room temperature; thus, temperature drop was due to the subjects' level of drowsiness alone. To make the findings of this research applicable for open environments, two solutions exist. First, one can measure the surrounding temperature regularly to calibrate facial temperature. Second, obtaining temperature differences between skin target areas just above the arteries and the areas far away from the arteries inherently removes the disturbance of the ambient temperature.

## Conclusion

Monitoring facial skin temperature by thermal imaging has the potential to detect drowsiness of drivers non-invasively. The results indicated that all subjects except one experienced facial skin temperature decline in three skin regions covering the three facial blood vessels from wakefulness to extreme drowsiness. The average temperature decline in the skin area covering the supratrochlear artery was as much as 0.54 ºC.

## Conflict of Interests

Authors have no conflict of interests.

## Acknowledgments

This paper is based upon a work supported by the Cognitive Science and Technology Council (CSTC) under Grant No. 1307.

## References

1. Barr L, Popkin S, Howarth H. An Evaluation of emerging driver fatigue detection measures and technologies. Scotts Valley, CA: CreateSpace Independent Publishing Platform; 2009.
2. Stutts JC, Wilkins JW, Scott OJ, et al. Driver risk factors for sleep-related crashes. Accid Anal Prev 2003; 35: 321-31.
3. Sahayadhas A, Sundaraj K, Murugappan M. Detecting driver drowsiness based on sensors: A review. Sensors (Basel) 2012; 12: 16937-53.
4. Sigari MH, Fathy M, Soryani M. A driver face monitoring system for fatigue and distraction detection. International Journal of Vehicular Technology 2013; 2013: 263983.
5. Ring EF. History of thermology and thermography: Pioneers and progress. Proceedings of the 12th EAT Congress on Thermology (EAT2012); 2012 Sep 5-8; Porto, Portugal.
6. . Wu S, Fang Z, Xie Z, et al. Blood perfusion models for infrared face recognition. In: Delac K, Editor. Recent advances in face recognition. London, UK: InTech Open; 2008. p. 183-206.
7. Gault TR, Blumenthal N, Farag AA, et al. Extraction of the superficial facial vasculature, vital signs waveforms and rates using thermal imaging. Proceedings of the 2010 IEEE Computer Society Conference on Computer Vision and Pattern Recognition; 2010 Jul 13; San Francisco, CA. p. 1-8.

8. Buddharaju P, Pavlidis IT, Tsiamyrtzis P, et al. Physiology-based face recognition in the thermal infrared spectrum. IEEE Trans Pattern Anal Mach Intell 2007; 29: 613-26.
9. Bando S, Oiwa K, Nozawa A. Evaluation of dynamics of forehead skin temperature under induced drowsiness. IEEJ Trans Elec Electron Eng 2017; 12: S104-S109.
10. Krauchi K, Cajochen C, Wirz-Justice A. A relationship between heat loss and sleepiness: effects of postural change and melatonin administration. J Appl Physiol (1985) 1997; 83: 134-9.
11. Gradisar M, Lack L. Relationships between the circadian rhythms of finger temperature, core temperature, sleep latency, and subjective sleepiness. J Biol Rhythms 2004; 19: 157-63.
12. Moradi S, Mansouri F, Sori F, et al. Sleepiness and changes in vital signs among the clinical shift workers staff at Imam Khomeini Hospital of Ilam. Int J Hosp Res 2014, 3: 19-24.
13. Wierwille WW, Ellsworth LA. Evaluation of driver drowsiness by trained raters. Accid Anal Prev 1994; 26: 571-81.
14. Perona P, Malik J. Scale-space and edge detection using anisotropic diffusion. IEEE Trans Pattern Anal Mach Intell 1990; 12: 629-39.
15. Philip RC, Ram S, Gao X, et al. A comparison of tracking algorithm performance for objects in wide area imagery. Proceedings of the 2014 Southwest Symposium on Image Analysis and Interpretation; 2014 Apr 6-8; San Diego, CA, USA. Piscataway, NJ: IEEE; 2014. p. 109-12.
16. Zhang K, Zhang L, Liu Q, et al. Fast visual tracking via dense spatio-temporal context learning. Proceedings of the Computer Vision-ECCV 2014: 13th European Conference, 2014 Sep 6-12; Zurich, Switzerland. Cham, Switzerland: Springer International Publishing; 2014. p. 127-41.
17. Ebrahimian Hadi Kiashari S, Nahvi A, Homayounfard A, et al. Monitoring the variation in driver respiration rate from wakefulness to drowsiness: A non-intrusive method for drowsiness detection using thermal imaging. J Sleep Sci. 3:1-9.
18. Benda NM, Eijsvogels TM, Van Dijk AP, et al. Altered core and skin temperature responses to endurance exercise in heart failure patients and healthy controls. Eur J Prev Cardiol 2016; 23: 137-44.